ICIC Express Letters
Part B: Applications
Volume **9**, Number **2**, February **2018**

ICIC International ©2018 ISSN 2185-2766
pp. 101–110

LOW-VOLTAGE AND LOW-POWER CHARGER CIRCUIT BASED ON A NOVEL SINGLE-SWITCH RESONANT CONVERTER WITH ZVS FOR USE IN PORTABLE EQUIPMENT

Ying-Chun Chuang[1,*], Hung-Shiang Chuang[2] and Cheng-Yi Chen[3]

[1]Department of Electrical Engineering
Kun Shan University
No. 195, Kun-Da Road, Yong-Kang District, Tainan City 71070, Taiwan
*Corresponding author: chuang@mail.ksu.edu.tw

[2]Guangdong-Taiwan College of Industrial Science and Technology
Dongguan University of Technology
No. 251, Xueyuan Road, Guancheng District, Dongguan 523000, P. R. China
c3479201@ms5.hinet.net

[3]Department of Electrical Engineering
Cheng Shiu University
No. 840, Cheng-Cing Road, Niao-Song District, Kaohsiung City 83347, Taiwan
k0464@gcloud.csu.edu.tw

Received August 2017; accepted November 2017

Abstract. *This paper develops a novel charger circuit for use in portable electronic equipment. The converter uses a single power switch to reduce the cost of the control circuit. The simple circuit configuration and few components provide desired circuit performance. With properly set circuit parameters, the power switch can be operated under the zero-voltage-switching (ZVS) condition, yielding a high circuit efficiency. A prototype circuit that is designed for a 6V-10Ah lead-acid battery is constructed and tested to confirm theoretical predictions. The measured maximum charging efficiency of the novel converter topology reaches 89.3%.*
Keywords: Charger circuit, Battery, Resonant converter, Zero-voltage switching

1. **Introduction.** Portable electronic equipment includes smart phones, laptop computers, personal digital assistants, telecom power supplies, cell phones, digital cameras, and so on [1]. Since portable electronic equipment continuously consumes electric energy from embedded rechargeable batteries, it requires charging circuits [2]. The charging time and lifetime of the rechargeable battery depend strongly on the properties of the charger circuit. For many years, most commercially available battery charger circuits have been linear-mode converters, in which an active power element regulates the output voltage. However, conventional battery chargers with linear power regulators can handle only low power, and have a very low efficiency, and a low power density, because they require low-frequency transformers and filters. Conversely, modern battery chargers are small, light, low-cost, and highly efficient in converting energy. Therefore, linear regulators have been increasingly replaced by high-efficiency switching DC-DC converters which have been advancing. Conventional DC-DC converters are large owing to the magnetic devices, which occupy most of their volume. However, in recent years, research into the miniaturization of magnetic devices has greatly advanced. Small DC-DC converter modules with soft switching for use in portable equipment have been developed. Both the zero-voltage-switching (ZVS) technique and the zero-current-switching (ZCS) technique are two commonly used soft-switching techniques, in which a resonant tank is used to realize soft-switching conditions.

Loaded-resonant converters are the most popular ZVS converters. According to how energy is extracted from a resonant tank, loaded-resonant converters can be classified as series-resonant, parallel-resonant, or series-parallel resonant converters. The series-resonant converter that is designed for a battery charger is the simplest, and it has many advantages [3,4]. Low-voltage active power switches can be used. Also, series-resonant converters can operate safely under no load because no current flows through their resonant circuits. Therefore, the series-resonant converter has the best topology for low-voltage and low-power battery charger applications in portable equipment because of its low switching losses, low stresses, and low noise characteristics among other advantages. The series-resonant converter is generally recommended for low-voltage and low-power battery charger applications because the energy conversion stage uses simple circuitry. The series-resonant converter and the class-E inverter were introduced in 1970 and in 1975, respectively [5,6]. The series resonant converter is the optimal topology for DC/DC energy conversion applications because it has many advantages, such as low switching losses, low stresses, and low noise characteristics. However, two active power switches connected to the input side of the resonant tank in a traditional series-resonant converter may increase the complexity of the trigger signal and control circuit. Additionally, the class-E resonant inverters are the most efficient inverters known to date. This work presents a novel battery charger circuit with an improved series-resonant converter, which integrates a traditional class-D series-resonant converter and a class-E resonant inverter, for rechargeable batteries for use in portable equipment. The proposed improved series-resonant converter outperforms the conventional class-D series-resonant converter with respect to size, weight, cost, simplicity of topology, and ease of control [7-9].

This paper is organized as follows. Section 2 describes the circuit, and analyzes the operation, of the novel single-switch resonant converter for use in portable equipment. Section 3 introduces the operating characteristics of the converter. Section 4 presents the implementation of the novel single-stage resonant converter and the results of its simulation. Finally, Section 5 draws conclusions.

2. Circuit Description and Operational Analysis.

2.1. Circuit description. The main shortcoming of the traditional series-resonant converter is that it has two active power switches and its generation of the trigger signals for the two power switches is a complex process. This topology is not suitable for low-power applications because the large number of components and complex control circuit increase cost and reduce reliability. Accordingly, many efforts have been made to find a less expensive low-voltage and low-power charger circuit topology for portable equipment to support competitive pricing for consumers. Figure 1 presents a basic diagram of a low-voltage and low-power battery charger with a novel single-switch resonant converter for portable equipment that meets the requirements of high efficiency and low cost. It comprises the power switch S with an antiparallel diode D and parallel capacitor C,

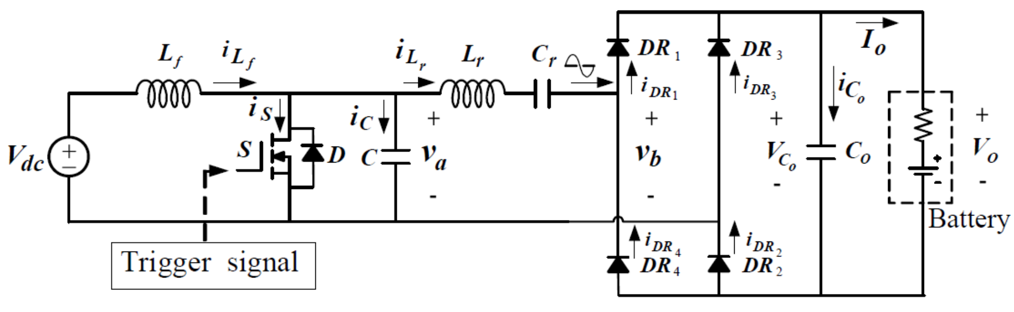

FIGURE 1. Proposed low-voltage and low-power battery charger

series-loaded resonant tank circuit L_r-C_r (resonating below the switching frequency of power switch S), and it passes a DC current input through the choke inductor L_f.

2.2. **Operational analysis.** This work proposes a novel zero-voltage switching technique. The objective of the proposed converter is to use auxiliary LC resonant elements to shape the voltage waveform of the switching device during the off time in to create a zero-voltage condition to turn the device on or off. Figure 2 presents interval transitions of the proposed single-switch resonant converter in one switching period.

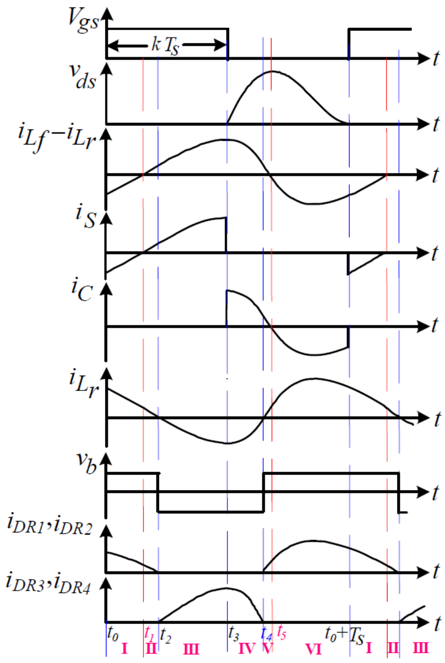

FIGURE 2. Voltage and current waveforms of novel single-switch resonant converter

For a steady-state cycle, the converter of Figure 1 operates in six intervals. The power switch S is assumed to be off before the first interval. The equivalent circuit in each switching interval transition of the proposed single-switch resonant converter is explained as follows.

Interval 1: (between t_0 and t_1)

In this interval, parallel capacitor voltage v_C falls to zero and a turn-on signal is applied to the gate of power switch S. Therefore, active power switch S turns on under zero-current-switching and zero-voltage-switching conditions. At the beginning of this interval, diode D conducts because the current i_{L_f}-i_{L_r} is negative. During the interval, rectifier diodes DR_1 and DR_2 are turned on because the resonant tank current i_{L_r} is positive; also, the input DC energy flows from the series resonant tank and through rectifier diodes DR_1 and DR_2 to charge the battery. Figure 3 presents the equivalent circuit of this mode. The circuit exits this mode as soon as diode D is reverse-biased by a positive current i_{L_f}-i_{L_r}.

Interval 2: (between t_1 and t_2)

At the beginning of this interval, the trigger signal is still applied to the gate of power switch S, which starts to turn on, and the capacitor voltage v_a is clamped at zero. Since diode D was conducting before power switch S was conducting, S is turned on at zero voltage, resulting in a zero turn-on loss for the power switch. Figure 4 presents the equivalent circuit. The line voltage is applied to L_f, and i_{L_f} increases continuously. In this interval, the current i_{L_f}-i_{L_r} naturally commutates from diode D to the active power switch S. The resonant current i_{L_r} passes through diodes DR_1 and DR_2 to charge the battery. Simultaneous conduction of diode DR_1 and switch DR_2 provides a positive voltage v_b, at the input terminal of the rectifier. The circuit operation enters Interval 3 when the inductor current i_{L_r} resonates and is negative.

Interval 3: (between t_2 and t_3)

At the beginning of this interval, the trigger signal has been applied to the gate of power switch S. Both currents i_{L_f} and i_{L_r} flow through the active power switch S. The resonant current i_{L_r} is now transferred to diodes DR_3 and DR_4 from diodes DR_1 and DR_2. In this interval, diodes DR_3 and DR_4 conduct and a negative voltage v_b appears at the input terminal of the rectifier. Figure 5 presents the equivalent circuit of this mode. This interval finishes when the power switch S is turned off.

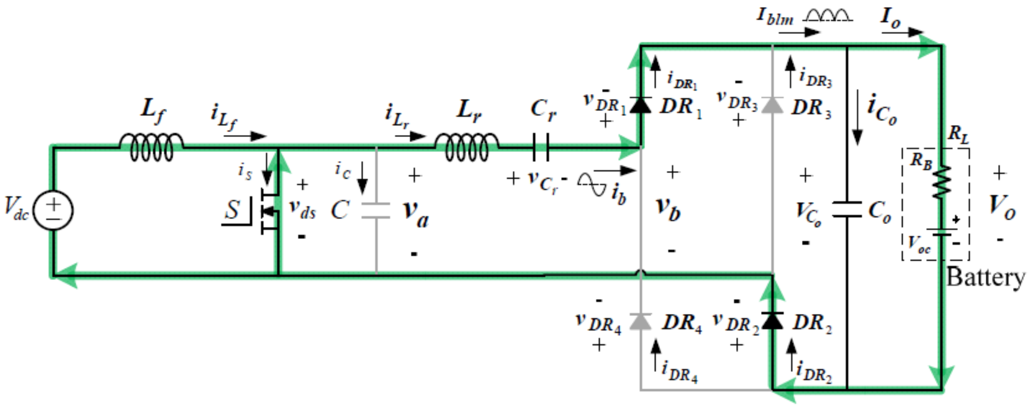

FIGURE 3. Equivalent circuit in Interval 1

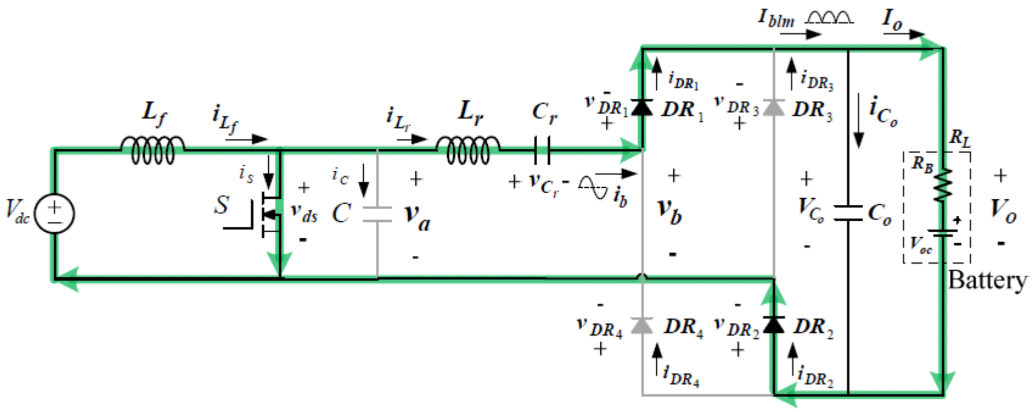

FIGURE 4. Equivalent circuit in Interval 2

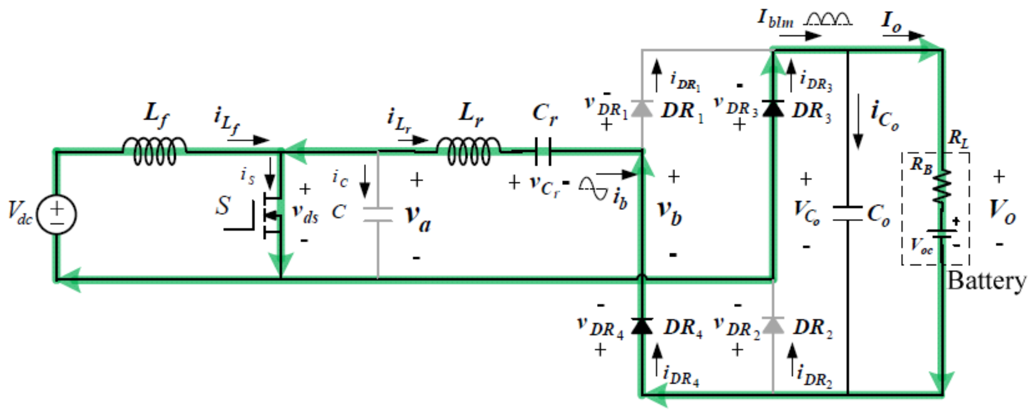

FIGURE 5. Equivalent circuit in Interval 3

Interval 4: (between t_3 and t_4)

At the beginning of this interval, a trigger signal from the gate of power switch S is removed. Power switch S begins to turn off, and the parallel capacitor C starts to charge. Simultaneously, owing to the negative resonant current i_{L_r}, the resonant circuit begins to charge the parallel capacitor C cross power switch S. Once the resonant current resonates to zero, Interval 5 begins. Figure 6 presents the equivalent circuit.

Interval 5: (between t_4 and t_5)

When the circuit enters Interval 5, the inductor current i_{L_r} is positive and the rectifier diodes DR_1 and DR_2 are turned on. In this time interval, the capacitor current i_c is still positive. Accordingly, the capacitor voltage v_c continues to increase to its peak value. Figure 7 presents the equivalent circuit. Interval 5 finishes at the time when i_c becomes zero, and then, the operating interval enters Interval 6.

Interval 6: (between t_5 and $t_0 + T_S$)

The capacitor current i_c which equals the difference between i_{L_f} and i_{L_r}, becomes negative in Interval 6. In this interval, the current i_{L_f}-i_{L_r} flows through capacitor C continuously. This interval finishes at the time when v_c resonates to zero. Figure 8 presents the equivalent circuit. When the active power switch S is again excited by the driving signal v_{gs}, this interval ends and the operation returns to Interval 1 of the next cycle. It should be noted that active power switch S is turned on under the ZVS condition.

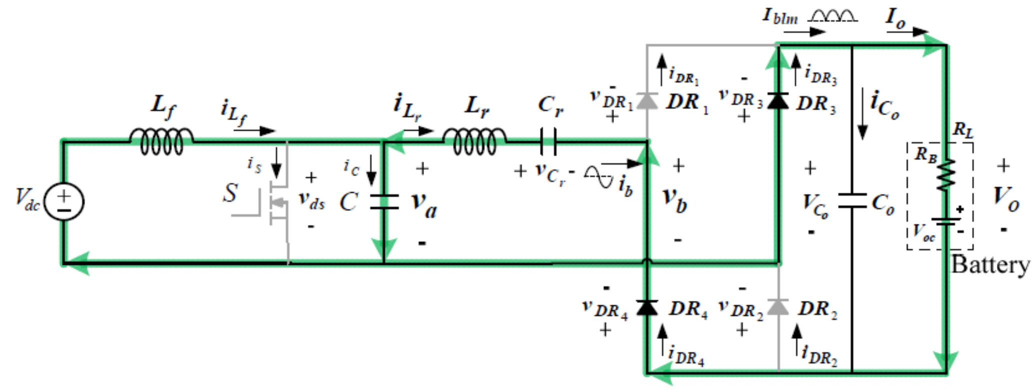

FIGURE 6. Equivalent circuit in Interval 4

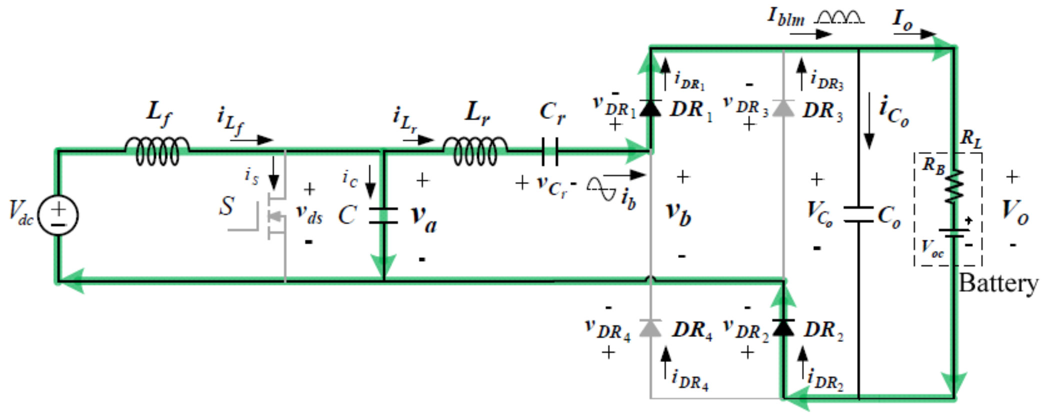

FIGURE 7. Equivalent circuit in Interval 5

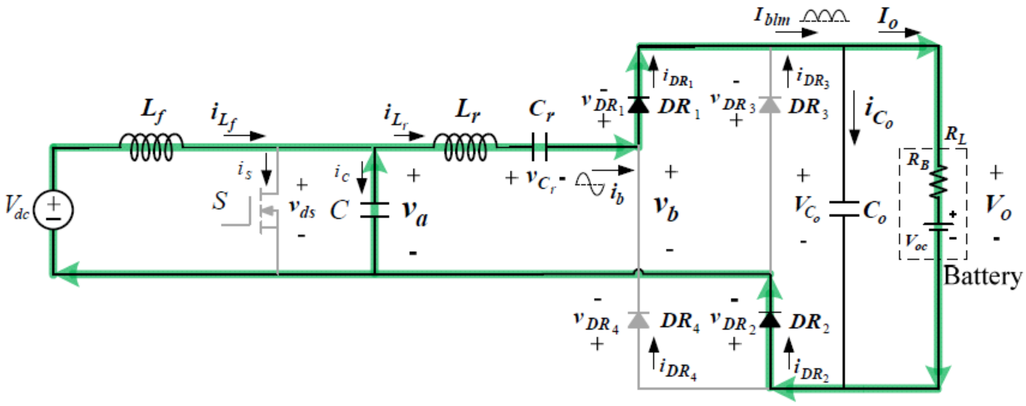

FIGURE 8. Equivalent circuit in Interval 6

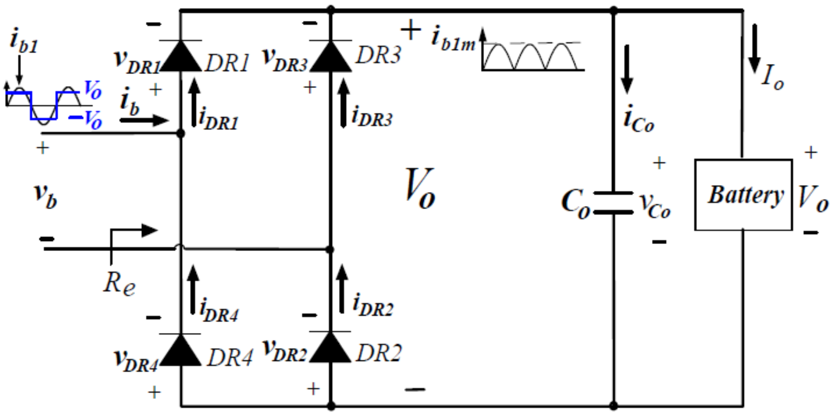

FIGURE 9. Simplified equivalent output stage of novel single-switch resonant converter

3. **Operating Characteristics.** Figure 9 illustrates the rectifier stage of the novel single-switch resonant converter of the output stage. Since the output voltage is assumed to be a constant V_O, the input voltage to the bridge rectifier, v_b, is V_O when i_{L_r} is positive and is $-V_O$ when i_{L_r} is negative.

The novel single-switch resonant converter with a bridge rectifier for battery charging applications is analyzed based on the fundamental frequency of the Fourier series of the voltages and currents. Then, the input voltage v_b of the bridge rectifier is given by the Fourier series in Equation (1).

$$v_b(t) = \sum_{n=1,3,5,\ldots}^{\infty} \frac{4V_O}{n\pi} \sin(n\omega t) \tag{1}$$

Equation (2) yields the fundamental component of voltage v_b.

$$v_{b1} = \frac{4V_O}{\pi} \sin(\omega t) \tag{2}$$

The inductor current i_{L_r} is approximated as a sine wave of amplitude $I_{L_{r1}}$, and then the average value of output current I_O is given by Equation (3).

$$I_O = \frac{2I_{L_{r1}}}{\pi} \tag{3}$$

The fundamental component of input current of the bridge rectifier is

$$I_{L_{r1}} = \frac{\pi I_O}{2} \tag{4}$$

The input resistance in this equivalent circuit of the bridge rectifier is determined from the ratio of voltage to current at the bridge rectifier. Equation (5) thus defines the input resistance.

$$R_e = \frac{V_{b1}}{I_{L_{r1}}} = \frac{8}{\pi^2} \cdot \frac{V_O}{I_O} \tag{5}$$

The relationship between input and output is approximately determined by performing an AC circuit analysis using the fundamental frequencies of the voltage and current. Figure 10 plots the equivalent AC circuit.

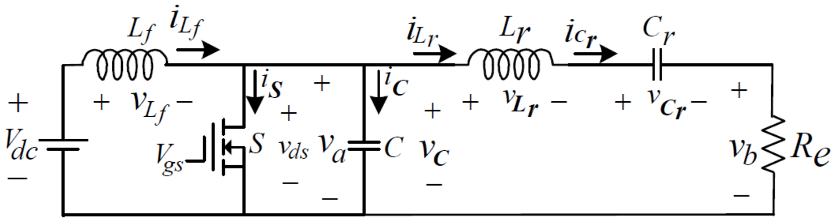

Figure 10. Equivalent AC circuit of novel single-switch resonant converter

The novel single-switch series resonant converter is characterized by two resonant frequencies, f_{o1} and f_{o2}. When the active power switch is on, the resonant frequency f_{o1} can be expressrd as Equation (6).

$$f_{o1} = \frac{1}{2\pi\sqrt{L_r C_r}} \tag{6}$$

When the active power switch is off, the resonant frequency f_{o2} is given by Equation (7).

$$f_{o2} = \frac{1}{2\pi\sqrt{L_r C_r C/(C_r + C)}} \tag{7}$$

To achieve zero-voltage switching of the active power stitch S, the operating frequency f_s should exceed the resonant frequency f_{o1}. To achieve resonant operation, the resonant circuit must be underdamped. That is

$$R_e \le 2\sqrt{\frac{L_r(C_r + C)}{C_r \cdot C}} \tag{8}$$

To satisfy both boundary conditions $v_c(2\pi) = 0$ and $i_S(2\pi) = 0$, the circuit parameters C_r, and L_r must meet the following equations.

$$C_r = \frac{2\sin(k\pi)\cos(k\pi+\phi)\sin(k\pi+\phi)[(1-k)\pi\cos(k\pi)+\sin(k\pi)]}{\omega R_e[\pi^2(1-k)]} \tag{9}$$

$$L_r = \frac{R_e\left\{2(1-k)^2\pi^2 - 1 + 2\cos(\phi)\cos(2k\pi+\phi) - \cos 2(k\pi+\phi)[\cos(2k\pi) - \pi(1-k)\sin(2k\pi)]\right\}}{4\omega\sin(k\pi)\cos(k\pi+\phi)\sin(k\pi+\phi)[(1-k)\pi\cos(k\pi)+\sin(k\pi)]} \tag{10}$$

where k is the duty cycle of the operation frequency and ϕ denotes the angular difference between the trigger signal v_{gs} and the resonant tank current i_{L_r}.

4. **Experimental Results.** To confirm the predicted operating principles and theoretical analysis of the proposed novel single-switch resonant converter low-voltage and low-power charger circuit applications, the laboratory converter in Figure 1 is designed and built to charge a 6V-10Ah lead-acid battery. The switching frequency is arbitrarily chosen to be 44kHz, which exceeds the range of frequencies that may generate acoustic noise. The circuit parameters are listed in Table 1. Circuit simulations are also performed using IsSpice software. A topology comparison between the proposed converter and traditional

class-D series-resonant converter is summarized in Table 2. Evidently, the proposed converter has the advantages of simple structure and easy control.

Figures 11(a) and 11(b) show the waveforms of the power switch. The measured experimental waveforms are highly quite consistent with the theoretical predictions. Figures 12(a) and 12(b) show the waveforms of the shunt capacitor. The experimental results shown in Figures 11 and 12 demonstrate that zero-voltage switching is achieved at constant frequency for the power switch. Figures 13(a) and 13(b) show the waveforms of input voltage v_b and current i_b of the bridge rectifier. The input voltage to the bridge rectifier v_b is V_O when i_{L_r} is positive and $-V_O$ when i_{L_r} is negative. Figures 14(a) and 14(b) show the measured voltage variation curve and charging current of the lead-acid battery during the charging period. Increasing the terminal voltage of the lead-acid battery from 5.7V to 8.1V took 270 minutes. The charging current I_O falls as the battery voltage V_O increases. Figure 15 shows the measured charging efficiency. The minimal and

TABLE 1. Circuit parameters

Input voltage V_{dc}	Resonant frequency f_{o1}	Choke inductor L_f	Shunt capacitor C
24V	20kHz	3mH	0.1μF
Duty cycle k	Switching frequency f_s	Resonant inductor L_r	Resonant capacitor C_r
0.48	44kHz	63μH	1μF

TABLE 2. Topology comparison between the proposed converter and traditional class-D series-resonant converter

	Number of power switch	Trigger signal	Number of input filter capacitor
The proposed converter	1	PWM trigger signal	0
Traditional class-D series-resonant converter	2	Two set of trigger signals with dead time and isolated circuit	2

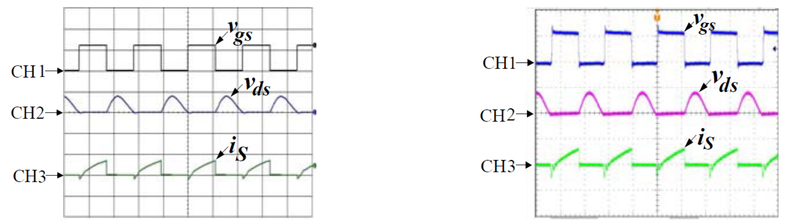

CH1: 10V/div CH2: 100V/div CH3: 5A/div Time: 10μs/div

(a) (b)

FIGURE 11. Trigger signal v_{gs} voltage v_{ds} and current i_S of power switch: (a) simulated waveforms, (b) measured waveforms

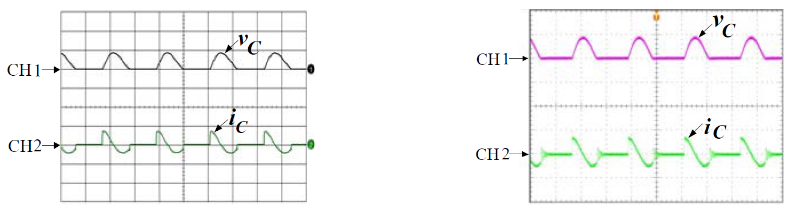

CH1: 100V/div CH2: 5A/div Time: 10μs/div

(a) (b)

FIGURE 12. Waveforms of shunt capacitor voltage v_C and current i_C: (a) simulated waveforms, (b) measured waveforms

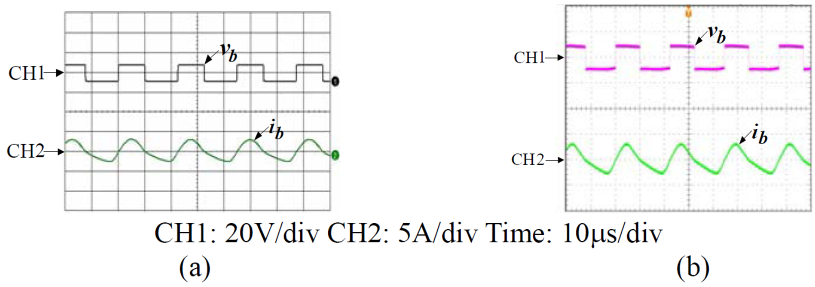

Figure 13. Waveforms of bridge rectifier input voltage v_b and current i_b: (a) simulated waveforms, (b) measured waveforms

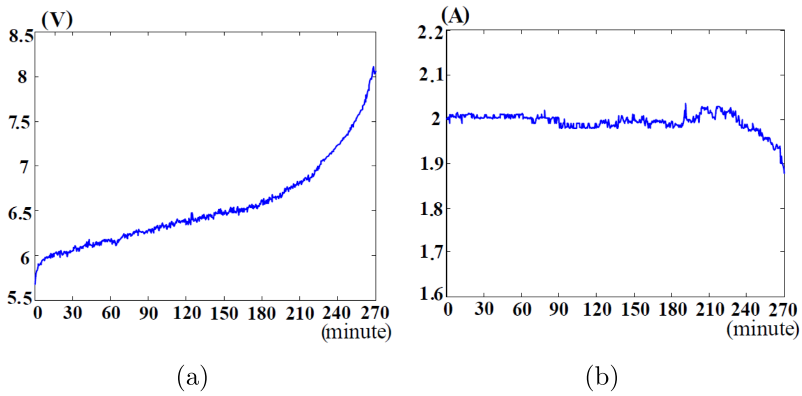

Figure 14. Measured battery terminal voltage and charging current during charging period: (a) battery terminal voltage, (b) charging current

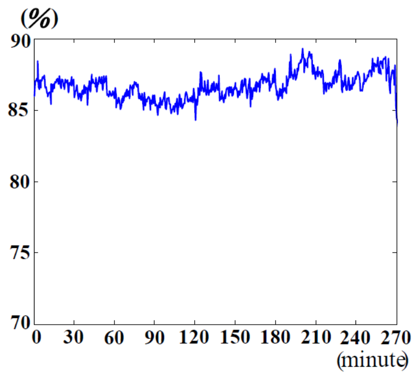

Figure 15. Measured charging efficiency during charging period

maximal efficiencies of the novel single-switch charging circuit were approximately 84.9% and 89.3%, respectively, and the total average charging efficiency during the charging of the novel single-switch battery charger circuit was 87.9%. A volume/weight comparison is summarized in Table 3 which shows that the proposed converter has the advantages of small size, light weight, and high efficiency. The proposed topology has great potential for low-voltage and low power charger circuit for use in portable equipment.

5. **Conclusions.** In this work, a novel single-switch resonant converter for low-voltage and low-power battery chargers was designed. Its circuit structure is simpler and cheaper than that of a traditional class-D resonant converter, which has many components. A battery charger with an improved single-switch series resonant topology was used in a charging test of a low-voltage and low-power lead-acid battery charger to demonstrate the effectiveness of the developed converter. The overall charging efficiency of the proposed

Table 3. Comparison between the proposed converter and traditional class-D series-resonant converter for use in battery charger circuit

	Dimension ($L \times W \times H$) (cm)	Weight (kg)	Minimal charging efficiency	Cost (USD)
The proposed converter	$10 \times 9 \times 4$	0.377	84.9%	23.8
Traditional class-D series-resonant converter	$12 \times 11 \times 4$	0.418	82.7%	27.9

converter exceeds 84.9%. Therefore, the charging efficiency can be improved using a novel single-switch series resonant converter and the ZVS technique. Favorable performance is obtained at a low cost and with few components.

REFERENCES

[1] S. Sugahara, K. Yamada, M. Edo, T. Sato and K. Yamasawa, Low power consumption and high power density integrated DC-DC converter for portable equipments, *IEEE Asian Solid-State Circuits Conference*, Fukuoka, Japan, pp.149-152, 2008.

[2] K. Eberts, Automatic charging methods for portable battery operated equipment, *IEEE Trans. Industrial Electronics and Control Instrumentation*, vol.IECI-12, no.2, pp.57-62, 1965.

[3] Y. C. Chuang, Y. L. Ke, H. S. Chuang and H. K. Chen, Implementation and analysis of an improved series-loaded resonant DC-DC converter operating above resonance for battery chargers, *IEEE Trans. Industry Applications*, vol.45, no.3, pp.1052-1059, 2009.

[4] Y. C. Chuang, H. S. Chuang, C. H. Yang and Y. S. Wang, A novel single-switch series resonant converter for low power DC/DC energy conversion applications, *2015 IEEE the 11th International Conference on Power Electronics and Drives Systems*, Sydney, Australia, pp.940-947, 2015.

[5] R. Redl, B. Molnar and N. O. Sokal, Small-signal dynamic analysis of regulated class E DC/DC converters, *IEEE Trans. Power Electronics*, vol.pe-1, no.2, pp.121-128, 1986.

[6] M. Mikolajewski and M. K. Kazimierczuk, Zero-voltage-ripple rectifiers and DC/DC resonant converters, *IEEE Trans. Power Electronics*, vol.8, no.1, pp.12-17, 1993.

[7] M. R. Amini and H. Farzanehfard, Switched resonator DC/DC converter with a single switch and small inductors, *IET Power Electronics*, vol.7, no.6, pp.1331-1339, 2014.

[8] J. Zeng, W. Qiao and L. Qu, A single-switch isolated DC-DC converter for photovoltaic systems, *2012 IEEE Energy Conversion Congress and Exposition*, pp.3446-3452, 2012.

[9] L. An and D. D. C. Lu, Design of a single-switch DC/DC converter for a PV-battery-powered pump system with PFM+PWM control, *IEEE Trans. Industrial Electronics*, vol.62, no.2, pp.910-921, 2015.